Observation of a Large Magnetic Anisotropy in the New 2H-Perovskite Related Oxide $Ba_8CoRh_6O_{21}$: Magnetic Measurements on Aligned Single Crystals

H.-C. zurLoye,* K. E. Stitzer, and M. D. Smith

Department of Chemistry and Biochemistry, University of South Carolina, Columbia, South Carolina 29208

A. El Abed[†] and J. Darriet

Institut de Chimie de la Matière Condensée de Bordeaux (ICMCB-CNRS), Avenue du Dr. Schweitzer, 33608 Pessac Cedex, France

Received February 26, 2001

Single crystals of $Ba_8CoRh_6O_{21}$, grown out of a potassium carbonate flux, were characterized by single-crystal X-ray diffraction and magnetic measurements. X-ray data were collected in a superspace group approach and solved using the JANA2000 software package. $Ba_8CoRh_6O_{21}$ represents the first example of a structurally characterized $m = 5$, $n = 3$ member of the $A_{3n+3m}A'_nB_{3m+n}O_{9m+6n}$ family of 2H hexagonal perovskite related oxides and contains chains consisting of six consecutive RhO_6 octahedra followed by one distorted CoO_6 trigonal prism. Magnetic measurements were carried out on large aligned single crystals, and a very large magnetic anisotropy in the magnetic susceptibility, persisting up to room temperature, was observed.

Introduction

Low-dimensional structures have historically attracted much interest due to the presence of magnetic behavior which is unique to structurally highly anisotropic systems.[1−3] Insights into such behavior can be gained from structural families where it is possible to systematically vary either the structure or the composition independently. For this reason, perovskite and perovskite-related oxides in particular have long provided excellent candidates for structural and physical property studies, due to the compositional and structural flexibility of this huge extended oxide family. Recently, much interest has focused on a large and varied group of oxides closely akin to the pseudo-one-dimensional 2H hexagonal perovskites, with the general formula $A_{3n+3m}A'_nB_{3m+n}O_{9m+6n}$ (n, m = integers, A = alkaline earth; A′, B = large assortment of metals including alkali, alkaline earth, transition, main group, and rare earth metals).[4−24] An early general structural classification of these materials based on the filling of interstitial sites generated by the stacking of $[A_3O_9]$ and $[A_3A'O_6]$ layers was developed by Darriet and Subramanian.[25,26] This approach easily describes the structural composition of all the commensurate members of this family of structures and can be extended to encompass members that form incommensurately modulated (aperiodic) structures.

An alternate, complementary description that highlights the low-dimensional nature of these compounds is the composite structure approach. In this structural description, these oxides consist of two crystallographically independent substructures, $[A]_\infty$ chains and $[(A',B)O_3]_\infty$ columns made up of distinct ratios of face-sharing octahedra and trigonal prisms. In many cases,

* To whom correspondence should be addressed. E-mail: zurloye@sc.edu.
[†] Mohamed I University, Facultédes Sciences, Oujda, Morocco.

(1) Schlenker, C.; Dumas, J. In *Crystal Chemistry and Properties of Materials with Quasi-One-Dimensional Structures, a Chemical and Physical Approach*; Rouxel, J., Ed.; Reidel Publishing Co.: Boston, 1986; p 135.
(2) de Jongh, L. J.; Miedema, A. R. *Adv. Phys.* **1974**, *23*, 1.
(3) Day, P. In *Solid State Chemistry Compounds*; Cheetham, A. K., Day, P., Eds.; Clarendon Press: Oxford, 1992; chapter 2.
(4) Nguyen, T. N.; Giaquinta, D. M.; zur Loye, H.-C. *Chem. Mater.* **1994**, *6*, 1642.
(5) Nguyen, T. N.; Lee, P. A.; zur Loye, H.-C. *Science* **1996**, *271*, 489.
(6) Fjellvåg, H.; Gulbrandsen, E.; Aasland, S.; Olsen, A.; Hauback, B. C. *J. Solid State Chem.* **1996**, *124*, 190.
(7) Kageyama, H.; Yoshimura, K.; Kosuge, K.; Mitamura, H.; Goto, T. *J. Phys. Soc. Jpn.* **1997**, *66*, 1607.
(8) Campá, J. A.; Gutiérrez-Puebla, E.; Monge, M. A.; Rasines, I.; Ruíz-Valero, C. *J. Solid State Chem.* **1994**, *108*, 230.
(9) Harrison, W. T. A.; Hegwood, S. L.; Jacobson, A. J. *J. Chem. Soc., Chem. Commun.* **1995**, 1953.
(10) Battle, P. D.; Blake, G. R.; Darriet, J.; Gore, J. G.; Weill, F. *J. Mater. Chem.* **1997**, *7*, 1559.
(11) Strunk, M.; Müller-Buschbaum, H. *J. Alloys Compd.* **1994**, *209*, 189.
(12) Dussarrat, C.; Fompeyrine, J.; Darriet, J. *Eur. J. Solid State Inorg. Chem.* **1995**, *32*, 3.
(13) Campá, J. A.; Gutiérrez-Puebla, E.; Monge, A.; Rasines, I.; Ruíz-Valero, C. *J. Solid State Chem.* **1996**, *126*, 27.
(14) Claridge, J. B.; Layland, R. C.; Adams, R. D.; zur Loye, H.-C. *Z. Anorg. Allg. Chem.* **1997**, *623*, 1131.
(15) Reisner, B. A.; Stacy, A. M. *J. Am. Chem. Soc.* **1998**, *120*, 9682.
(16) Blake, G. R.; Sloan, J.; Vente, J. F.; Battle, P. D. *Chem. Mater.* **1998**, *10*, 3536.
(17) Huvé, M.; Renard, C.; Abraham, F.; Van Tendeloo, G.; Amelinckx, S. *J. Solid State Chem.* **1998**, *135*, 1.
(18) Boulahya, K.; Parras, M.; González-Calbet, J. M. *J. Solid State Chem.* **1999**, *142*, 419.
(19) Smith, M. D.; zur Loye, H.-C. *Chem. Mater.* **2000**, *12*, 2404.
(20) Irons, S. H.; Sangrey, T. D.; Beauchamp, K. M.; Smith, M. D.; zur Loye, H.-C. *Phys. Rev. B* **2000**, *61*, 11594.
(21) Zakhour-Nakhl, M.; Claridge, J. B.; Darriet, J.; Weill, F.; zur Loye, H.-C.; Perez-Mato, J. M. *J. Am. Chem. Soc.* **2000**, *122*, 1618.
(22) Layland, R. C.; zur Loye, H.-C. *J. Alloys Compd.* **2000**, *299*, 118.
(23) Layland, R. C.; Kirkland, S. L.; zur Loye, H.-C. *J. Solid State Chem.* **1998**, *139*, 79.
(24) Smith, M. D.; Stalick, J. K.; zur Loye, H.-C. *Chem. Mater.* **1999**, *11*, 2984.
(25) Darriet, J.; Subramanian, M. A. *J. Mater. Chem.* **1995**, *5*, 543.
(26) Perez-Mato, J. M.; Zakhour-Nakhl, M.; Weill, F.; Darriet, J. *J. Mater. Chem.* **1999**, *9*, 2795.

10.1021/ic010222d CCC: $20.00
Published on Web 08/24/2001

the ratio of the repeat distances of the two chains is not a rational number, and, consequently, the structure is incommensurately modulated along the chain direction. As shown previously, a better structural formulation of such composites is $A_{1+x}(A'_xB_{1-x})O_3$, where $x = n/(3m+2n)$ and ranges continuously between 0 and 1/2, corresponding to chains containing all face-shared octahedra and alternating face-sharing octahedra and trigonal prisms, respectively.[26−28] For simple fractional values of x, such as 1/5, 2/7, or 1/3, the structure is commensurate and the end-members, the 2H perovskite ($BaNiO_3$, $x = 0$) and the K_4CdCl_6 ($x = 1/2$) structure types, are well known.

Most structural and physical property measurements of these compounds (and oxides in general) have been carried out on polycrystalline samples,[29,30] as oxide single-crystal growth is often unsuccessful. Recently, however, the application of single-crystal flux-growth techniques has enabled the growth of large, high-quality single crystals of this family of oxides,[31−33] which has made possible precise structural determination of both commensurate and incommensurate compounds, and promises to offer a deeper insight into these materials.[34] We have discussed a four-dimensional superspace group approach in recent papers,[21,26] and further detailed explanations of the composite structure approach and its description using the superspace formalism can be found in several papers and references therein.[35−39]

In addition to providing the best possible structural information, single crystals, if suitably large, are ideal for performing magnetic measurements, especially if the magnetic behavior varies as a function of crystal orientation relative to an applied magnetic field.[31,34] In this paper we report the structure determination and aligned single-crystal magnetic measurements of a new commensurate member of this family of oxides, $Ba_8CoRh_6O_{21}$, which exhibits a very large magnetic anisotropy.

Experimental Section

Crystal growth: Flux synthesis; Rh powder (0.20 g; Engelhard, 99.5%), Co_3O_4 (0.24 g; Johnson-Matthey, 99.99%), $BaCO_3$ (1.16 g; Alfa, 99.99%), and K_2CO_3 (15.8 g; Fisher, reagent grade) were mixed thoroughly and placed in an alumina crucible. The filled crucible was covered and heated in air from room temperature to the reaction temperature of 1050 °C at 600 °C h^{-1}, held at 1050 °C for 12 h, and cooled at 12 °C h^{-1} to 875 °C, at which point the furnace was turned off and the system allowed to cool to room temperature. The flux was removed with water and the crystals isolated manually.

Structure Determination. Data collection was performed on an Enraf-Nonius CAD4 diffractometer (Mo Kα) in the supercell approach. The unit cell parameters of both subsystems were determined precisely, and refinements led to the following values: $a = 10.0431(1)$ Å, $c_1 = 2.5946(1)$ Å, and $c_2 = 4.5405(1)$ Å. With the [(Co, Rh)O_3] subsystem as the reference system, the modulation wave vector is defined by $\mathbf{q} = \gamma\mathbf{c_1}^*$, where $\gamma = c_2^*/c_1^* = c_1/c_2 = 0.57143(1)$. The γ value of 0.57143(1) is a rational fraction (4/7, corresponding to $x = 1/7$) and corresponds to a commensurate chain sequence of one trigonal prism and six octahedra, with an overall composition of $A_8A'B_6O_{21}$. The first and second subsystems are related to the (3+1)D superspace group by the application of the W_1 and W_2 transformation matrices, respectively:

$$W_1 = \begin{vmatrix} 1 & 0 & 0 & 0 \\ 0 & 1 & 0 & 0 \\ 0 & 0 & 1 & 0 \\ 0 & 0 & 0 & 1 \end{vmatrix} \quad W_2 = \begin{vmatrix} 1 & 0 & 0 & 0 \\ 0 & 1 & 0 & 0 \\ 0 & 0 & 0 & 1 \\ 0 & 0 & 1 & 0 \end{vmatrix}$$

The two possible superspace groups that are compatible with the observed extinction conditions of $-h + k + l \neq 3n$ for (h, k, l, m) and $m \neq 2n$ for (h, 0, l, m) are $R3m(00\gamma)0s$ and the corresponding centrosymmetric superspace group $R\bar{3}m(00\gamma)0s$. $R\bar{3}m(00\gamma)0s$ was chosen initially and confirmed by the successful solution of the structure. Final R values: $R = 0.0532$ ($R_w = 0.0590$) for all reflections; $R = 0.0418$ ($R_w = 0.0459$) for 499 main reflections; $R = 0.0712$ ($R_w = 0.0700$) for 927 satellites of order 1; and $R = 0.0692$ ($R_w = 0.0964$) for 171 satellites of order 2.

Scanning Electron Microscopy. Scanning electron micrographs of several single crystal samples were obtained using a Hitachi 2500 Delta SEM. The crystals were sputtered with gold to prevent charging. The SEM also verified the presence of Ba, Co, and Rh as the only metals in all crystals.

Magnetic Susceptibility. Magnetic susceptibility of powder samples of $Ba_8CoRh_6O_{21}$ as a function of temperature was measured using a Quantum Design MPMS XL SQUID magnetometer, at applied field strengths of 5 and 40 kG. Both field-cooled (FC) and zero-field cooled (ZFC) measurements were performed in the temperature range 2 K ≤ T ≤ 300 K. The sample was contained in a gelatin capsule fastened in a plastic straw for immersion into the SQUID. No diamagnetic correction was made for the sample container.

Aligned single-crystal measurements were performed using a Quantum Design Single-Crystal Rotator attachment. A large single crystal was affixed to the crystal rotator using standard vacuum grease and immersed in the SQUID magnetometer. The crystal rotator enables continuous in-situ measurements of magnetization as a function of crystal orientation relative to the applied field. After centering the crystal in the instrument, the susceptibility was measured as a function of crystal orientation. The crystal is rotated in 10° steps through 360°. Knowing the initial orientation of the crystal makes it possible to determine if the maximum or minimum susceptibility position corresponds to the c axis of the crystal being oriented parallel or perpendicular to the applied magnetic field. For collecting the data of the temperature dependence of the susceptibility, a crystal was mounted on a straw with the crystal orientation set to correspond to either the maximum or the minimum susceptibility position. With the position fixed, the susceptibility is then measured as a function of temperature. This procedure is repeated for both the parallel and the perpendicular crystal orientation.

Results and Discussion

Plentiful black hexagonal rodlike single crystals of $Ba_8CoRh_6O_{21}$ ranging in size from submillimeter to ~7 mm in length were grown from a molten potassium carbonate flux. Figure 1 is an image of several crystals obtained from the flux, showing the variability in size and aspect. The larger specimens are typical of those used for the aligned single-crystal magnetic measurements (see below). For the structure determination, a small crystal was chosen. The X-ray intensity data were collected in the supercell approach. Data reduction, absorption corrections (ψ scan), and transformation of the indices were carried out using the JANA 2000 program

(27) Evain, M.; Boucher, F.; Gourdon, O.; Petricek, V.; Dusek, M.; Bezdicka, P. *Chem. Mater.* **1998**, *10*, 3068.
(28) Gourdon, O.; Petricek, V.; Dusek, M.; Bezdicka, P.; Durovic, S.; Gyepesova, D.; Evain, M. *Acta Crystallogr.* **1999**, *B55*, 841.
(29) Kageyama, H.; Yoshimura, K.; Kosuge, K.; Azuma, M.; Takano, M.; Mitamura, H.; Goto, T. *J. Phys. Soc. Jpn.* **1997**, *66*, 3996.
(30) Aasland, S.; Fjellvåg, H.; Hauback, B. *Solid State Commun.* **1997**, *101*, 187.
(31) Claridge, J. B.; Layland, R. C.; Henley, W. H.; zur Loye, H.-C. *Chem. Mater.* **1999**, *11*, 1376.
(32) Henley, W. H.; Claridge, J. B.; Smallwood, P. L.; zur Loye, H.-C. *J. Cryst. Growth* **1999**, *204*, 122.
(33) zur Loye, H.-C.; Layland, R. C.; Smith, M. D.; Claridge, J. B. *J. Cryst. Growth* **2000**, *211*, 452.
(34) Maignan, A.; Michel, C.; Masset, A. C.; Martin, C.; Raveau, B. *Eur. Phys. J.* **2000**, *B15*, 657.
(35) van Smaalen, S. *Phys. Rev. B* **1991**, *43*, 11330.
(36) Janner, A.; Janssen, T. *Acta Crystallogr.* **1980**, *A36*, 399.
(37) Janner, A.; Janssen, T. *Acta Crystallogr.* **1980**, *A36*, 408.
(38) Perez-Mato, J. M.; Madariaga, G.; Zuñiga, F. J.; Garcia Arribas, A. *Acta Crystallogr.* **1987**, *A43*, 216.
(39) van Smaalen, S. *Cryst. Rev.* **1995**, *4*, 79.

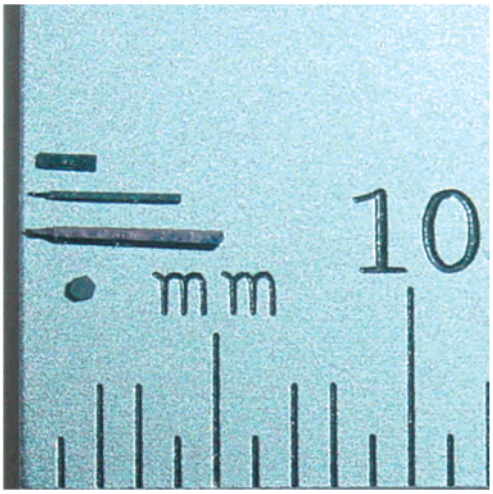

Figure 1. Flux-grown single crystals of $Ba_8CoRh_6O_{21}$. The larger specimens are similar to the crystal used for aligned magnetic measurements; the small crystal shown is of a typical size used for the structure determination.

Table 1. Fractional Atomic Average Coordinates and Equivalent Isotropic Displacement Factors

Subsystem [(Co, Rh)O_3]: $R\bar{3}m(00\gamma)0s$

atom	x_0	y_0	z_0	U_{eq}(Å^2)
Co	0	0	0	0.033(1)
Rh	0	0	0	0.0078(2)
O	0.1545(3)	0.1545(3)	1/2	0.019(1)

Subsystem [Ba]: $P\bar{3}c1(001/\gamma)$

atom	x_0	y_0	z_0	U_{eq}(Å^2)
Ba1	0.32561(9)	0	1/4	0.0119(4)
Ba2	0.3491(2)	0	1/4	0.0059(5)

package.[40,41] The atomic coordinates for the two subsystems are given in Table 1.

An approximate [110] view of the composite structure of $Ba_8CoRh_6O_{21}$ is shown in Figure 2. The repeat sequence in the face-shared polyhedral $[(A',B)O_3]_\infty$ subsystem consists of six consecutive RhO_6 octahedra followed by one distorted CoO_6 trigonal prism. The metal−oxygen bond distances (ranges: Co−O = 2.184(1)−2.197(1) Å; Rh−O = 1.905(1)−2.055(1) Å) are typical for oxides of this type. Intrachain Co−Rh (2.755(1) and 2.777(1) Å) and Rh−Rh (ranging between 2.497-(1) and 2.546(1) Å) distances are short but nonbonding.[42] $Ba_8CoRh_6O_{21}$ represents the first example of a structurally characterized $m = 5$, $n = 3$ member of the $A_{3n+3m}A'_nB_{3m+n}O_{9m+6n}$ family and one of only a small number of compositions other than $n = 1$ and $m = 0$ that remain in a commensurate form. Importantly, the synthesis and successful structure determination of $Ba_8CoRh_6O_{21}$ further establishes the validity of the general structural classification developed by Darriet and Subramanian.[25,26] Reports in the literature claim the existence of several other commensurate members of this family based on TEM studies of powder samples.[18] However, these typically lack

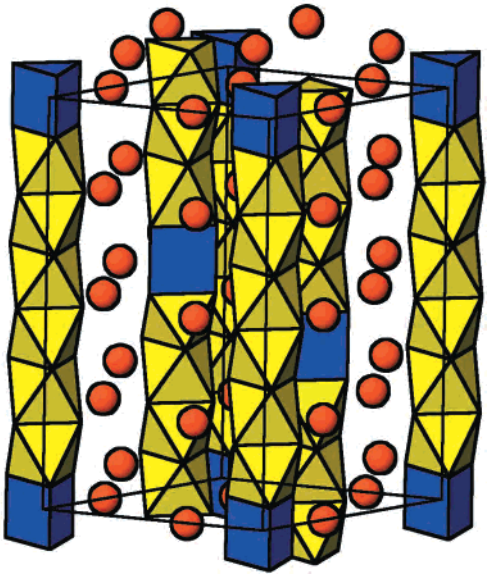

Figure 2. Approximate [110] view of the structure of $Ba_8CoRh_6O_{21}$. yellow, RhO_6 octahedra; blue, CoO_6 trigonal prisms; red, Ba atoms.

detailed structural characterizations of the materials under investigation, such as atomic coordinates based on Rietveld refinement of powder data and, typically, compositional claims are based on nominal starting compositions.

There are several possible formal oxidation state distributions for cobalt and rhodium in $Ba_8CoRh_6O_{21}$, and one might expect that the bond valence approach could help with the assignment of these oxidation states. A calculation of bond valences for rhodium and cobalt using the bond valence parameters given by N. E. Brese and M. O′Keefe[43] for Co^{2+} and Rh^{3+} leads to a value of 1.56 for cobalt and ∼3.5 for rhodium. If one uses the bond valence parameter for Rh^{4+} instead, the resultant bond valence of rhodium is closer to that of Rh^{4+}.

The value obtained for cobalt deviates slightly from Co^{2+}; however, the bond valence parameter used for this cation (1.692) corresponds to an octahedral or tetrahedral environment, which may not be consistent with the value for the unusual trigonal prismatic coordination of cobalt observed in this phase. Unfortunately, there is no example to our knowledge from which to deduce the bond valence parameter of the trigonal prismatic environment (the stacking of the oxygen atoms is not the same as that for octahedra or tetrahedra). Consequently, one consistent assignment of oxidation states for this compound is as follows: one Co^{2+} and six Rh^{4+}. (Alternatively, although less likely, another possibility that cannot be excluded at present is one Co^{3+}, one Rh^{3+}, and five Rh^{4+}.) Further clarification of the oxidation states will await planned XANES experiments.

The availability of large single crystals presents a great opportunity to carry out magnetic measurements on oriented single crystals. While there exists an extensive literature on anisotropic magnetic materials and the determination of their magnetic behavior using single crystals,[1,2] this is typically not the case for this family of oxides. Anisotropies have been predicted for these pseudo-one-dimensional materials, and the most in-depth investigations have been carried out on $Ca_3Co_2O_6$, an $n = 1$, $m = 0$ member of this family, using polycrystalline samples[29,30] and more recently, single crystals.[34]

For the magnetic measurements of $Ba_8CoRh_6O_{21}$, a large single crystal 3.5 mm in length and weighing 2.85 mg was used. Though unsuitably large for a single-crystal structure determination, the crystal system and unit cell parameters of this crystal were determined on a Bruker SMART APEX CCD single

(40) Petricek, V.; Dusek, M. *JANA2000: Programs for Modulated and Composite Crystals*; Institute of Physics: Praha, Czeck Republic, 2000.
(41) Dusek, M.; Petricek, V.; Wunschel, M.; Dinnebier, R. E.; van Smaalen, S. *J. Appl. Crystallogr.*, submitted for publication.
(42) Vajenine, G. V.; Hoffmann, R.; zur Loye, H.-C. *Chem. Phys.* **1996**, *204*, 469. Extended Hückel calculations on related systems (Sr_3NiPtO_6, Sr_3NiIrO_6, and Sr_3CoPtO_6) indicate very narrow metal bands, suggesting a lack of direct, or for that matter, oxygen-bridge-mediated, metal−metal interactions.

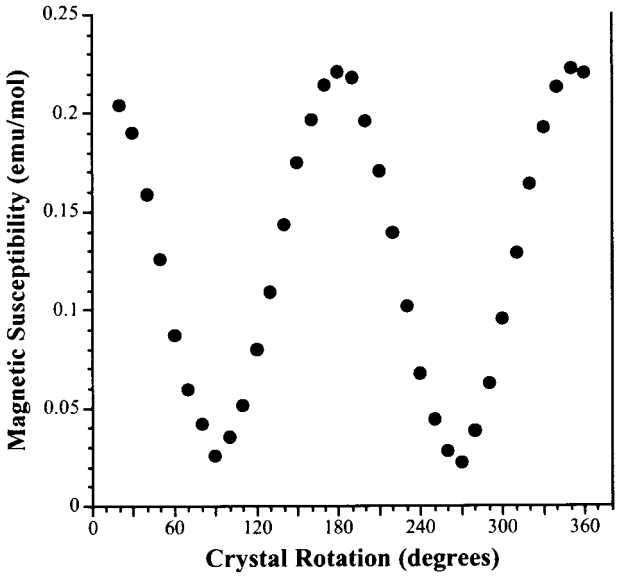

Figure 3. Magnetic susceptibility of a single crystal of $Ba_8CoRh_6O_{21}$ as a function of crystal orientation with respect to the applied magnetic field measured at 2 K and 5 kG. The maxima occur for the crystal *c* axis aligned parallel with the applied field.

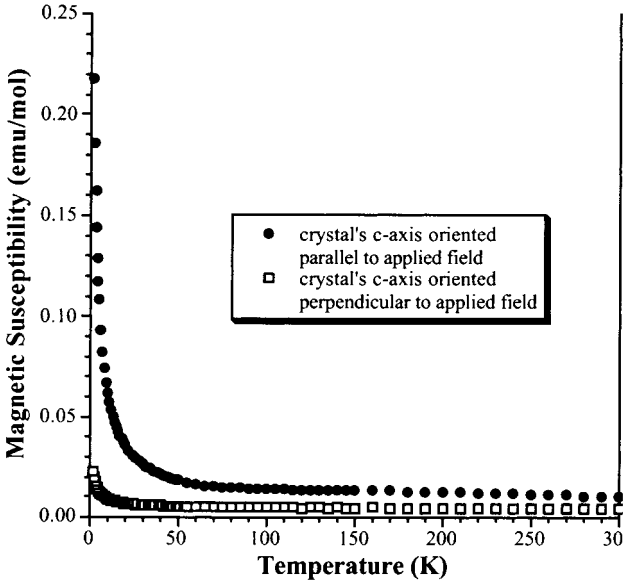

Figure 4. Temperature dependence of the magnetic susceptibility of a single crystal of $Ba_8CoRh_6O_{21}$ oriented parallel (closed circles) and perpendicular (open squares) with respect to the applied field of 5 kG.

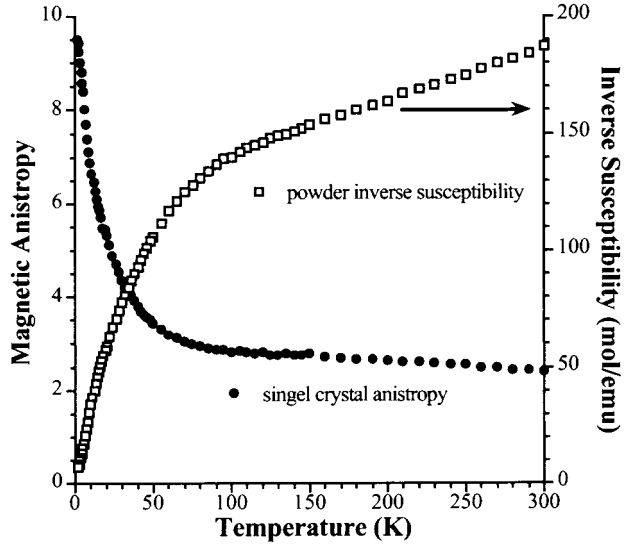

Figure 5. Correlation between the magnetic anisotropy (defined as the ratio between the susceptibility of a single crystal of $Ba_8CoRh_6O_{21}$ oriented parallel and perpendicular with respect to the applied field) with the inverse susceptibility of $Ba_8CoRh_6O_{21}$ powder as a function of temperature at 5 kG. The onset of the increase in the magnetic anisotropy occurs in the same temperature region as the decrease in the inverse susceptibility, indicating a strong correlation.

crystal diffractometer after the magnetic measurements were performed and shown to be identical to those used for the structure solution. The crystal was affixed to a Quantum Design crystal rotator device to characterize the magnetization of the crystal as a function of orientation relative to the applied field. Figure 3 plots the magnetic susceptibility of the single crystal as a function of crystal orientation, at 2 K. A beautiful, regular sinusoidal variation in the susceptibility is clearly evident. The maxima in the susceptibility correspond to a parallel alignment of the hexagonal *c* axis (i.e., the $[CoRh_6O_{21}]_\infty$ chain direction) with the applied field, and the minima correspond to a 90 degree rotation from that position or a perpendicular orientation of the *c* axis relative to the magnetic field. A large magnetic anisotropy is clearly evident, with a ratio of M(parallel)/M(perpendicular) $\sim$ 10 at 2 K. The magnitude of this anisotropy is demonstrated by Figure 4, which shows the temperature dependence of the magnetic susceptibility of the single crystal as a function of crystal alignment. It can be seen that the magnetic anisotropy persists all the way up to room temperature and beyond.

These measurements demonstrate the importance of carrying out magnetic measurements on single crystals, at least for this rhodium family of oxides. Measurements using powder samples will necessarily yield an averaged result that depends on the magnitude of the magnetic anisotropy. For example, Figure 5 compares the single crystal anisotropy with the inverse susceptibility measured on a randomly oriented polycrystalline sample of $Ba_8CoRh_6O_{21}$, which was obtained by grinding a sample of single crystals to a fine powder. The previously unexplained behavior of the powder inverse susceptibility is clearly correlated with the large increase in the single-crystal anisotropy beginning in the 100−50 K range, suggesting that both are caused by the same magnetic interactions present in the sample.

The anisotropy up to room temperature can be rationalized by the intrinsic anisotropy of both Rh^{4+} and Co^{2+}. If one speculates that the intrachain exchange interaction is relatively strong due to the relatively short Rh−Rh distance (≈2.5 Å), then the very large observed θ value of −550 K[44] can be explained by a first-order spin−orbit contribution to the magnetism of Rh^{4+} and Co^{2+}. The Curie constant obtained from high-temperature susceptibility data (150−300 K) of $C = 4.5$ emu K mol^{-1} is not very different from the value calculated for six spins of $S = 1/2$ plus one spin of $S = 3/2$ (4.1 emu K mol^{-1}).[45]

The temperature dependence of the magnetic anisotropy is undoubtedly more complex in nature. When approaching the three-dimensional ordering temperature (below 2 K), we expect the spin correlation length to increase; therefore, the increasing anisotropy between the perpendicular and parallel susceptibilities

(43) Brese, N. E.; O'Keeffe, M. *Acta Crystallogr.* **1991**, *B47*, 192.

(44) Fitting the high-temperature data (150−300 K) of the inverse susceptibility from Figure 5 yields $C = 4.5$ emu K mol^{-1} and $\theta = -550$ K.

(45) A Curie constant of 4.90 emu K mol^{-1} is expected for one Co^{3+}, one Rh^{3+}, and five Rh^{4+}.

may have a contribution from an anisotropy of the exchange interaction within or between the chains, in addition to any intrinsic anisotropy of both Rh^{4+} and Co^{2+}. Future, very high temperature magnetic susceptibility measurements, combined with XANES data, are needed to definitively establish the oxidation states of the metals and to gain a better understanding of the magnetism of the system.

The existence of such an anisotropy has been hypothesized previously in Sr_3CuIrO_6,[46] where due to the lack of suitably large single crystals it has not been possible to conclusively demonstrate its existence. It is interesting to note, however, that $Ba_8CoRh_6O_{21}$ displays such a large anisotropy, persisting up to and beyond room temperature, even though there are no clear indications of long-range magnetic correlations evident in the temperature dependence of the magnetic susceptibility. Furthermore, it seems reasonable to assume that this type of magnetic anisotropy is not unique to the $Ba_8CoRh_6O_{21}$ or $Ca_3Co_2O_6$ members of this family. In fact, similar results have been observed for related rhodium oxides, which will be reported soon.

Acknowledgment. Financial support from the National Science Foundation through Grant DMR:9873570 is gratefully acknowledged.

Supporting Information Available: Crystallographic data in CIF format. This material is available free of charge via the Internet at http://pubs.acs.org.

IC010222D

(46) Nguyen, T. N.; zur Loye, H.-C. *J. Solid State Chem.* **1995**, *117*, 300.